PARSIFAL: parametrized simulation of triple-GEM and micro-RWELL response to a charged particle

R. Farinelli[1,*] on behalf of the working group

[1]INFN, Sezione di Ferrara, via G. Saragat 1, 44122 Ferrara, Italy

Abstract. PARSIFAL (PARametrized SImulation) is a software tool that can reproduce the complete response of both triple-GEM and micro-RWELL-based trackers. It takes into account the involved physical processes by their simple parametrization and thus in a very fast way. Existing software such as GARFIELD++ is robust and reliable, but CPU time-consuming. The implementation of PARSIFAL was driven by the necessity to reduce the processing time, without losing the precision of a complete simulation. A series of parameters, that can be extracted from the GARFIELD++ simulation, are set as input to PARSIFAL, which then runs independently from GARFIELD++. PARSIFAL can simulate samples with high statistics much faster, taking into account the various steps (ionization, diffusion, multiplication, signal induction, and electronics) from the simple sampling from parameterized distributions. In the case of the micro-RWELL MPGD, the effect of the high resistivity layer on the charge spread on the anode was introduced, following M.S. Dixit and A. Rankin's treatment. PARSIFAL was used to simulate triple-GEM chambers and the results were tuned to match experimental data from testbeams. In this case, the adopted electronics was APV-25 readout by SRS system, which has been simulated in the code. The same procedure was later applied to micro-RWELL chambers, readout by the TIGER ASIC and the GEMROC system. These new electronics were added to PARSIFAL code, and the simulated-to-real data was tuned. A presentation of the full code will be given in this contribution, setting the focus on the latest implementations and a first comparison with experimental data from micro-RWELL.

1 Introduction

Gaseous detectors are complex instruments employed to determine one or multiple characteristics of charged particles for both experimental and applied physics purposes. For instance, triple-GEM detectors are utilized in the CMS forward muon system [1], while trackers are employed in imaging and dosimetry for applications in hadrontherapy [2]. The underlying physics mechanism for detection is a shared principle among gaseous detectors: when a charged particle enters the gaseous volume, ionization occurs. The resulting primary electrons are then drifted towards a region of high electric field, where signal amplification generates a detectable current pulse.

This study will center on the Micro Pattern Gaseous Detector (MPGD) family. The origin of MPGD can be traced back to the development of Micro-Strip Gas Chambers (MSGC) [3].

*e-mail: rfarinelli@fe.infn.it

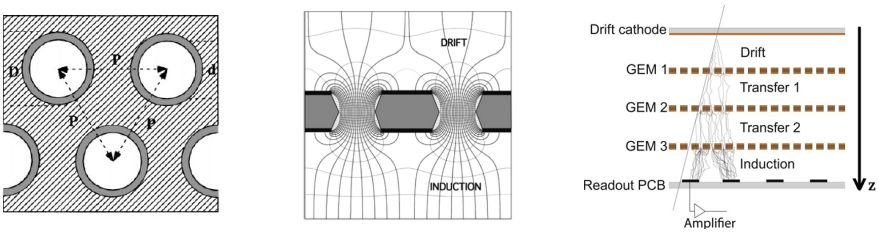

Figure 1. Scheme of a GEM foil from top (*left*) and side (*middle*): the holes have a pitch $p = 140\,\mu m$, and a bi-conical shape with inner diameter $d = 50\,\mu m$ and outer diameter $D = 70\,\mu m$. The copper thickness on the two sides t is 5 μm and the polyimide thickness of the bulk T is 50 μm [5]. A high voltage difference is applied between the copper layers and the electric field lines generated inside the holes are shown in the *middle* plot [6]. A schematic drawing of a typical triple-GEM detector configuration, which consists of a cathode, three stages of GEM, and an anode for the signal readout, segmented in strips or pads is shown in the *right* figure.

MSGC integrates patterning methodologies derived from the semiconductor sector, including photolithography and etching, to establish an intensely focused electric field for signal amplification and a optimized layout for signal readout.

After the evolution of MSGC, novel structures emerged, incorporating diverse amplification approaches using micro-electrodes (such as MicroGap, MicroDot, Micro-Groove) or partially uniform electric fields (for example, MICROMEGAS, GEM, μ-RWELL). The main features of the MPGDs include high spatial resolution, high particle-flux capability, large active areas with small dead surfaces, and resilience to radiation.

The technologies under study in the next paragraphs will be *triple-GEM* and μ*-RWELL*.

1.1 Triple-GEM technology

In 1997, F. Sauli introduced the Gaseous Electron Multiplier (GEM) [4]. This innovation involves a polyimide foil, 50 μm thick and coated with a 5 μm layer of copper on both sides. The foil contains a densely arranged pattern of holes, each having a diameter of 50 μm and spaced at a pitch of 140 μm (shown in Figure 1, on the left and in the middle). By applying a potential difference of a few hundred volts between the two copper-coated sides, an electric field of approximately 50 kV/cm is generated within the holes.

Upon entry into a hole, a primary electron accelerates and excites neighboring gas molecules, consequently initiating an electron avalanche amplification. To attain the desired gain value, several amplification stages are stacked, each subjected to a lower voltage. This approach minimizes the discharge probability when compared to a single GEM stage. Figure 1 on the right shows the triple-GEM structure [5].

1.2 μ-RWELL technology

The μ-RWELL [7] is a resistive MPGD: compact, spark protected, and with a single amplification stage. This amplification stage, along with the readout system, is built up by a multilayer Printed Circuit Board (PCB). For amplification, a 50 μm polyimide foil, featuring a high-density arrangement of 50 μm holes, is employed. One side of the foil is copper-coated (resembling the GEM foil structure), while the opposing side bears a thin layer of Diamond-Like-Carbon (DLC) achieved through sputtering. This DLC layer not only provides resistive properties to serve as spark protection but also facilitates charge dispersion [8]. The full detector scheme is given by the PCB described above, the cathode, and the gas volume.

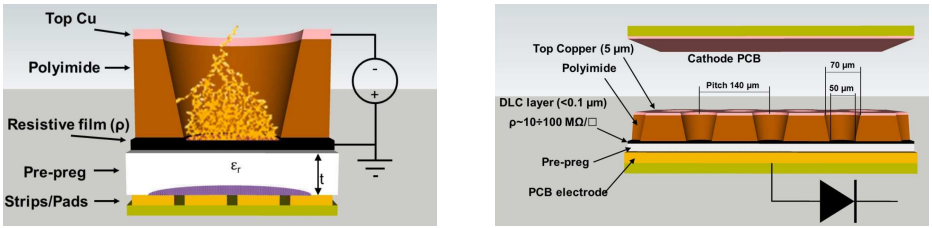

Figure 2. Scheme of a μ-RWELL PCB from side (*left*) and the μ-RWELL detector (*right*): the holes have a pitch $p = 140\,\mu$m, with inner diameter $d = 50\,\mu$m and outer diameter $D = 70\,\mu$m. The copper thickness on the top sides t is 5 μm and the polyimide thickness of the bulk T is 50 μm. A high voltage difference is applied between the copper layer and the DLC and the intense electric field generates the electron cascade if primary electrons enter the hole. A schematic drawing of a typical μ-RWELL detector configuration, which consists of a cathode and PCB is shown in the *right* figure.

Table 1. Detectors setting defined through the testbeam campaigns.

	Triple-GEM	μ-RWELL
amplification stages	3	1
gas mixture	Ar:iC_4H_{10} (90:10)	Ar:CO_2:CF_4 (45:15:40)
ionization gas gap	5 mm	6 mm
other gaps	2 mm	none
drift fields	1.5 kV/cm	3.5 kV/cm
transfer field	3 kV/cm	none
induction field	5 kV/cm	none
amplification voltage	250-280 V (x3)	450-650 V
DLC resistivity	none	20-80 MΩ/□
readout layout	strip 2D	strip 1D
readout pitch	650 μm	400 μm
electronics	APV-25/SRS	APV-25/SRS

2 Detector characterization

Numerous testbeam campaigns have been conducted to comprehensively characterize both of these technologies across various configurations and settings. The purposes are to understand the physical processes involved in signal generation and establish the most effective operational configurations. The primary objective behind these MPGDs is to precisely measure particle positions. The main goal of these campaigns is to enhance spatial resolution and optimize detector efficiency.

The testbeam took place in the SPS North Area at CERN with a muon or pion beam with 150 GeV/c momentum. The detector configurations are described in Table 1 and the achieved results are reported in the literature [9–11].

3 Detector simulation

A software tool capable of precisely modeling the response of a detector system and conducting performance calculations proves to be immensely invaluable during both the design and optimization phases of the detector, as well as throughout an ongoing experiment, particularly for generating Monte Carlo samples. Ensuring that these simulations closely mirror the

experimental measurements is of paramount importance, as it guarantees their reliability in predicting the behavior of the detector across various settings and adjustments.

The most widespread and robust existing software for gaseous detector simulation is GARFIELD++, defined as *"an object-oriented toolkit for the detailed simulation of particle detectors which use a gas mixture or a semiconductor material as sensitive medium"* [12].

Simulating an MPGD using this tool demands significant CPU time. For studies necessitating high statistical accuracy, it becomes imperative to reduce computation time by multiple orders of magnitude. This research is dedicated to crafting an accelerated MPGD simulation tool named PARSIFAL. The objective is to achieve a CPU time reduction of approximately three orders of magnitude, accomplished through two techniques.

Firstly, the simulation of the complete detector is segmented into distinct and autonomous tasks, such as diffusion and amplification. This division allows for parallel processing and accelerates the simulation. Secondly, the approach revolves around dissecting each distinct physical process and parameterizing it suitably for detector simulation. This method enables the simulation to concentrate on specific aspects of the simulation.

The sum of parameterized processes defines PARSIFAL as software for trustworthy and fast simulations of MPGD detectors. The code is scripted in C++, following an Object-Oriented paradigm, and necessitates only the ROOT framework [13] for installation and compilation procedures. The parameter initialization process is carried out by simulating the individual processes independently, using GARFIELD++.

Within PARSIFAL, three processes—ionization, electron drift, and amplification are parametrized from GARFIELD++. Conversely, other processes like charge dispersion, induction, and electronics are based on existing models.

Through its adept integration of these methods and capabilities, PARSIFAL emerges as a robust tool capable of swiftly simulating MPGD detectors with high fidelity.

3.1 Ionization

Ionization represents the initial stage in the detection of charged particles. During this phase, interactions with gas atoms result in the generation of primary electrons, and in certain instances, secondary electrons if the kinetic energy is sufficiently high. The process's parametrization depends on two key variables: the probability of producing a primary electron within a 1 cm path and the probability of generating any secondary electrons. This obviates the need to compute the cross-section for particle-gas interactions at each simulation step. Furthermore, due to the Poissonian nature of ionization, the distribution of electrons along the particle's trajectory can be easily established using the extracted variables. These two variables depend only on the gas mixture and the particle energy.

3.2 Electron drift

Primary and secondary electrons are accelerated by the electric field toward the amplification regions. Multiple factors contribute to determining the eventual position of each electron, with the primary ones being the gas composition and the electromagnetic field. These factors establish attributes such as transverse and longitudinal diffusion, drift velocity, Townsend coefficient, and Penning transfer rate.

Given a fixed configuration the factors above are defined. As a result, an electron's ultimate position after its drift depends only on its initial position. A parametrization of the mean displacement and positional dispersion is conducted as a function of the electron's initial position to parameterize the electron drift. This approach eliminates the need to calculate

electron scattering and gas interactions at each simulation step. Instead, the final position (or time) is determined by smearing based on the four extracted variables, simplifying the process while retaining accuracy.

3.3 Signal amplification

The signal amplification establishes the number of electrons generated per primary electron and is influenced by two factors: the transparency of the GEM (or WELL) foil and its gain. Transparency signifies the likelihood of an electron entering an amplification hole (and exiting in the case of a GEM foil). This process is the most resource-intensive aspect in terms of CPU time. The distribution of detector gain is extracted from GARFIELD++ and subsequently utilized as a parameter within PARSIFAL.

In scenarios where conducting a high-statistics GARFIELD++ simulation proves challenging, a Polya function can be employed to define the probability distribution of electron gains. This approach provides an alternative means of approximating gain distribution, accommodating situations where GARFIELD++ simulations might not be feasible with the desired level of statistical accuracy.

3.4 Charge dispersion

Charge dispersion arises due to the presence of a resistive layer within the μ-RWELL detector, acting as a dielectric spacer. When the charge is deposited, it disperses across the resistive layer, leading to an enlarged area being influenced by the amplified signal from the detector. A model describing the charge dispersion phenomenon is described in [14]. This model is subsequently tailored to the specific readout scheme employed, as outlined in Eq. 1, wherein the evolution of charge density is defined as a function of both spatial and temporal variables.

$$Q(t) * \int_{x1}^{x2} \rho(x,t)dx = \frac{q}{2}\left[erf\left(\frac{x_2 - x_0}{\sqrt{(}2)\sigma_0(1+\frac{t-t_0}{\tau})}\right) - erf\left(\frac{x_1 - x_0}{\sqrt{(}2)\sigma_0(1+\frac{t-t_0}{\tau})}\right)\right]\Theta(t-t_0) \quad (1)$$

where x_1 and x_2 are the strip boundaries, σ_0 is the hole dimension, and τ is the time constant of the resistive layer together with the readout plane.

3.5 Induction

Electron motion within the detector results in the generation of a time-varying current, as described by the Shockley-Ramo theorem [15, 16]. However, employing this approach can prove computationally intensive. To enhance computational efficiency, PARSIFAL employs a simplified induction model for comparison. In this simplified approach, the total induced charge on a single strip corresponds to the cumulative number of electrons that effectively interact with the readout.

Given that the induction time (a few nanoseconds) is notably shorter than the timescale for the induction of all electrons generated within the detector (tens of nanoseconds), PARSIFAL simulates induction by applying a 1.6 fC/ns pulse once the electrons reach the readout. A comparison is conducted between this simplified approach and the one based on the Shockley-Ramo theorem. The outcomes of the two methods are found to be consistent, affirming the effectiveness of the simplified induction model.

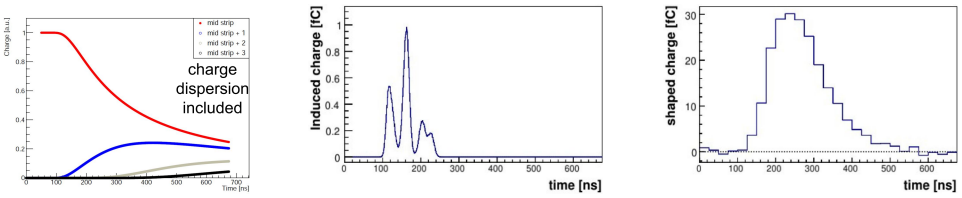

Figure 3. Signal generation steps in PARSIFAL: charge dispersion (*left*), induction (*middle*) and electronics (*right*). On the left, the evolution of the charge induced on a strip is reported: the charge moves from a strip to the neighbors. In the middle and the right figures, it is shown the current pulse induced on a strip in a simulated event of a triple-GEM detector, while on the right the output of the APV-25 electronics with a shaping time of 50 ns and a sampling of the charge each 25 ns.

.

3.6 Electronics

The electronics are described with a simplified approach. The induced current is integrated and convoluted with the Eq. 2 that reproduces a simplified RC-CR circuit of the shaper. The charge is sampled each 25 ns as performed by the APV-25 electronics.

$$f_{shaper}(t) = \frac{t - t_0}{\tau} \exp\left(-\frac{t - t_0}{\tau}\right), \tag{2}$$

where t_0 is the arrival time of the electron to the readout and τ is the shaping time of the APV-25.

4 Results

The events generated through PARSIFAL's simulations have undergone analysis using methodologies identical to those applied to experimental data [17]. Four key variables have been selected to quantify the quality of the simulation results: the total charge collected and the number of strips fired to characterize the shape of the signal recorded on the readout; charge centroid and μTPC spatial resolution to determine the precision of the reconstruction algorithms. These four selected variables collectively provide a comprehensive evaluation of the simulation's fidelity and effectiveness in replicating the experimental outcomes. To improve the matching been experimental data and simulation, some parameters have been tuned to reach a good matching. This also allows us to overcome some limitations in GARFIELD++ and PARSIFAL. The variables chosen to be tuned are the following: spatial diffusion of the electrons, gain of the GEM foil, and resistivity of the μ-RWELL.

Results are shown in Fig. 4 and 5. The agreement between the simulation results and experimental data, falling within the experimental uncertainties, serves to validate PARSIFAL as a reliable tool for conducting high-statistic MPGD simulations. As demonstrated, PARSIFAL's versatility extends to accommodating diverse geometry configurations, varying high voltage settings, and distinct gas mixtures. This flexibility positions PARSIFAL as an instrumental resource for comprehensively simulating various MPGD scenarios with substantial statistical accuracy.

References

[1] CMS Collaboration, The Phase-2 Upgrade of the CMS Muon Detectors, CERN-LHCC-2017-012, CMS-TDR-016 (2017), https://cds.cern.ch/record/2283189.

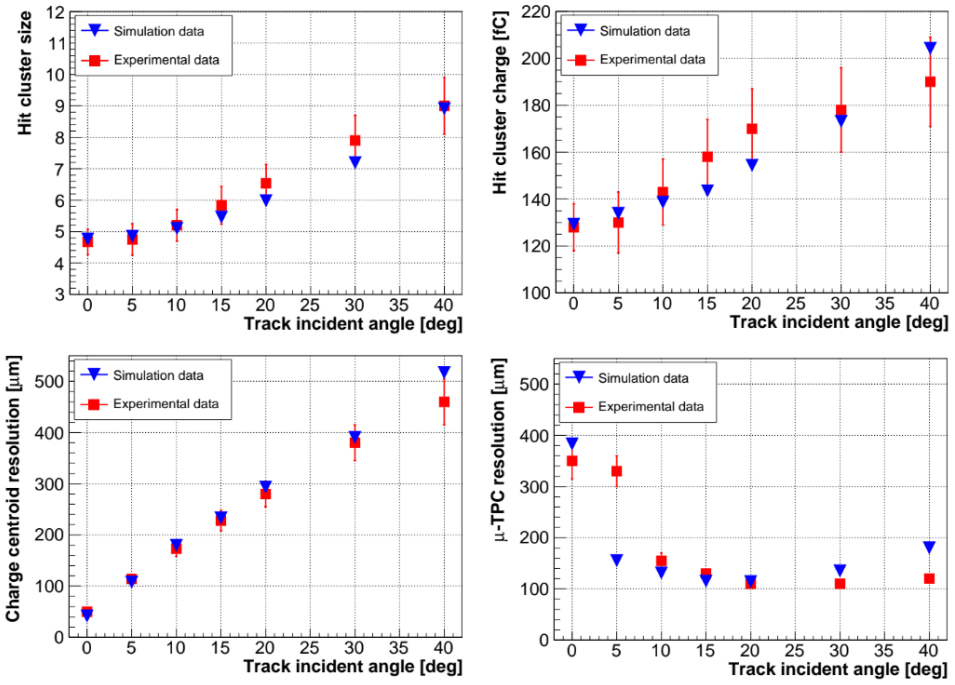

Figure 4. Simulated (*blue triangles*) and experimental (*red squares*) data for the four variables of interest as a function of the incident angle: on top the number of strip fired (*left*) and total charge collected (*right*), on bottom the spatial resolution for Charge Centroid algorithm (*left*) and µTPC (*right*).

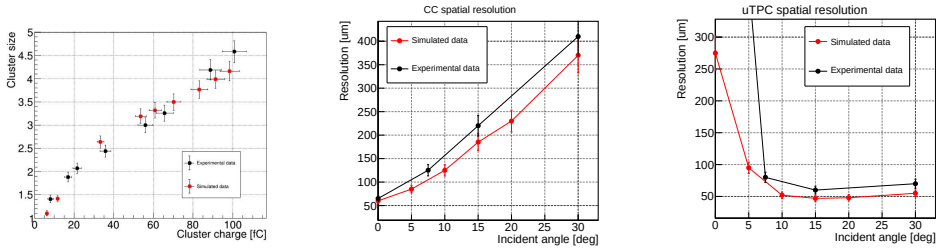

Figure 5. 123

.

[2] https://www.sciencedirect.com/science/article/abs/pii/S0168900212011813?via

[3] A. Oed. “Position-sensitive detector with microstrip anode for electron multiplication with gases”. Nucl. Instr. Meth. A263 (1988), pp. 351–359.

[4] F. Sauli, "GEM: A new concept for electron amplification in gas detectors", Nucl. Instr. and Meth. A386 (1997), pp. 531-534", doi:10.1016/S0168-9002(96)01172-2

[5] S. Bachmann *et al.*, "Charge amplification and transfer processes in the gas electron multiplier", Nucl. Instr. and Meth. A438 (1999), pp. 376-408, doi:10.1016/S0168-

9002(99)00820-7

[6] F. Sauli, "The gas electron multiplier (GEM): Operating principles and applications", Nucl. Instr. and Meth. A805, (2016), pp. 2-24, doi:10.1016/j.nima.2015.07.060

[7] G. Bencivenni *et al.*, "The micro-Resistive WELL detector: a compact spark-protected single amplification-stage MPGD", *J. Instrum.* **10** (2015) P02008, doi:10.1088/1748-0221/10/02/p02008

[8] M. S. Dixit *et al.*, "Position sensing from charge dispersion in micro-pattern gas detectors with a resistive anode", Nucl. Instrum. Methods Phys. Res. A518 (2004), pp 721-727, doi:10.1016/j.nima.2003.09.051

[9] I. Balossino *et al.*, "The CGEM-IT: An Upgrade for the BESIII Experiment", *Symmetry* **2022**, 14, 905. doi: 10.3390/sym14050905

[10] G. Bencivenni *et al.*, "On the space resolution of the μ-RWELL, J. of Instrumentation 16 (08)100 (2021) P08036, doi:10.1088/1748-0221/16/08/p08036

[11] R. Farinelli *et al.*, "The μ-RWELL technology at the IDEA detector", PoS ICHEP2022, (2022) 333, doi:10.22323/1.414.0333

[12] R. Veenhof, "GARFIELD, recent developments", Nucl. Instr. and Meth. A419, (1998) pp. 726-730, doi:10.1016/S0168-9002(98)00851-1

[13] https://root.cern.ch/

[14] M. S. Dixit *et al.*, "Simulating the charge dispersion phenomena in Micro Pattern Gas Detectors with a resistive anode", Nucl. Instrum. Methods Phys. Res. A566 (2006), pp 281, doi:10.1016/j.nima.2006.06.050

[15] W. Shockley, "Currents to conductors induced by a moving point charge", J. Appl. Phys. 9, 10 (1938) pp. 635, doi:10.1063/1.1710367

[16] S. Ramo, "Currents Induced by Electron Motion", Proc. of the IRE 27, 9 (1939) pp. 584—585, doi:10.1109/JRPROC.1939.228757"

[17] R. Farinelli, "Research and development in cylindrical triple-GEM detector with μTPC readout for the BESIII experiment", 2019 JINST TH 002.